1050 *Macromolecules* **2010**, *43*, 1050–1060
DOI: 10.1021/ma9020664

Macromolecules
ARTICLE

Surface Assembly of Catechol-Functionalized Poly(L-lysine)-*graft*-poly(ethylene glycol) Copolymer on Titanium Exploiting Combined Electrostatically Driven Self-Organization and Biomimetic Strong Adhesion

Sina Saxer,[†] Cyril Portmann,[‡] Samuele Tosatti,[†] Karl Gademann,[‡] Stefan Zürcher,*[,†] and Marcus Textor[†]

[†]*Laboratory for Surface Science and Technology, Department of Materials, Swiss Federal Institute of Technology (ETH Zurich), 8093 Zurich, Switzerland, and* [‡]*Chemical Synthesis Laboratory, SB-ISIC-LSYNC, Swiss Federal Institute of Technology (EPFL), 1015 Lausanne, Switzerland*

Received September 16, 2009

ABSTRACT: Nonfouling coatings, based on surface-tethered, hydrophilic polymer chains, have widespread application in areas such as biosensing, medical devices, and biotechnology. Self-organization of polymers is a particularly attractive approach given its simplicity and cost-effectiveness in the application. Here we present a new class of polymers based on the polycationic poly(L-lysine)-*graft*-poly(ethylene glycol) copolymer (PLL-*g*-PEG) with a fraction of the amine-terminated lysine side chains covalently conjugated to 3,4-dihydroxyphenylacetic acid (DHPAA). This copolymer is shown to adsorb and self-organize as a confluent monolayer on negatively charged titanium oxide surfaces, driven by long-range electrostatic attraction, while the catechol groups of DHPAA spontaneously engage in strong, coordinative binding to the substrate surface, similar to the biomimetic dihydroxyphenylalanine (DOPA) found in mussel adhesive proteins. The adsorption kinetics and resulting polymer coverage are demonstrated to critically depend on (a) a rational design of the copolymer architecture with a compromise between sufficient positive charges in the PLL backbone and a minimal grafting density of DHPAA groups and (b) optimum choice of ionic strength and temperature of the assembly solution. PLL-*graft*-(DHPAA; PEG) adlayers exhibit excellent resistance to nonspecific protein (fibrinogen) adsorption. To test the chemical stability of the polymeric layer, coated substrates were exposed to high ionic salt solutions and proved to remain nonfouling thanks to stable catechol−substrate anchorage, in stark contrast to the control PLL-*g*-PEG copolymer that desorbed under these conditions as a consequence of screening of the (purely) electrostatic surface forces. Furthermore, polymer-coated substrates resisted attachment of the cyanobacterium *Lyngbya sp.* over a time frame of at least 100 days.

Introduction

Techniques to modify substrate surfaces are key for many industrial and research applications ranging from corrosion and wear protection to biocompatibility of materials and biomedical devices to biosensors and drug delivery systems.[1−5] The toolbox of methods available today covers a large number of approaches with their specific advantages and limitations. Examples include plasma and electrochemical deposition or conversion, grafting-from and grafting-to polymeric systems, and chemical and physical vapor deposition, among others.[6,7] Spontaneous self-assembly and organization of designed molecules and polymers, incorporating adhesion and other functions, are particularly attractive as they constitute cost-effective, easy-to-upscale techniques, applicability to large areas and three-dimensional devices of complex shape, and conformity (for thin films) with micro- and nanoscale surface topologies, while requiring only minimal amounts of materials. Examples include self-assembled monolayers of alkanethiols on gold and silver[8,9] and alkanephosphates and phosphonates on metal oxides,[10−15] electrostatically driven deposition of polyelectrolytes as monolayers[16] or multilayers,[17] Langmuir−Blodgett (LB) films,[18] and functional silanes.[19,20]

There is a need, though, for adding to this existing toolbox since many techniques suffer from specific drawbacks such as substrate specificity (e.g., alkanethiols for gold and silver substrates mostly, phosphates for metal oxides only), requirement of advanced or expensive equipment (LB films), and limited stability or lifetime (e.g., oxidation of thiol surface linker, hydrolysis of silanes, instability of polyelectrolytes at interfaces in the presence of high salt media, and exchange processes of such polyelectrolytes with biomolecules in solution).

For a number of applications in biotechnology and biomedical engineering, surface modifications are required that suppress undesirable nonspecific adsorption of biomolecules such as proteins, glycoproteins, and lipids as well as attachment of eukaryotic cells or bacteria.[3,21,22] Frequently used polymers that provide such passive, "nonfouling" properties include poly(vinylpyrrolidone) (PVP),[23] poly(2-methyl-2-oxazoline) (PMOXA),[24] and, in particular, poly(ethylene glycol) (PEG).[25,26] These are uncharged, hydrophilic, strongly hydrated polymers, a combination of properties usually considered as a prerequisite for nonfouling functionality.[27] Additionally, interfacial architecture of the polymers is essential, and high chain surface density ("brush regime") has been demonstrated to be a key to general resistance against protein adsorption in contact with complex media such as blood serum.[28]

Selected grafting techniques have been demonstrated to be efficient in achieving high chain surface densities, in particular so-called "cloud point grafting" exploiting the inverse temperature−solubility properties of PEG.[27] Typically, PEG that is functionalized with a surface-active group such as a silane is grafted to the

*Corresponding author: Fax +41 (44) 801 80 60; Tel +41 (44) 801 80 50; e-mail stefan.zuercher@mat.ethz.ch.

 Published on Web 10/19/2009

substrate surface in high-salt, aqueous media and at temperatures that are below but close to the cloud point temperature, where PEG has lost part of its hydration layer, resulting in a reduced radius of gyration. High polymer chain surface densities can thus be achieved and, upon return to standard, e.g., physiological, conditions, PEG chains become rehydrated and swell, forming a brush monolayer that shows improved resistance to protein adsorption.

Another useful approach that has been developed by our group uses PEG-grafted polyelectrolyte copolymers that assemble, through electrostatic interaction, to oppositely charged surfaces, e.g., poly(L-lysine)-*graft*-poly(ethylene glycol), PLL-*g*-PEG, and thus provide fairly densely packed, confluent monolayers on negatively charged surfaces (e.g., tissue-culture polystyrene (TCPS), silica and glass, as well as many metal oxides such as titanium and niobium oxide). These ultrathin films resist unspecific protein adsorption when exposed to full blood serum at a level below the detection limit of optical, label-free techniques such as OWLS and SPR (< 2 ng/cm^2).[16,29] They are stable and functional for days to weeks (at neutral pH), depending on the application conditions (e.g., 21 days resistance to cell attachment in serum-complemented cell culture medium[30]), but slowly degrade with time and desorb rapidly at high ionic strength as well as low or high pH.[31]

More recently, adhesives found in nature have attracted wide interest and are now exploited in synthetic approaches. An example is mussel adhesive proteins (MAPs)[32] that allow mussels to adhere at high binding strength and under wet conditions to a large variety of materials. The Messersmith group was first to exploit this concept for the fabrication of nonfouling surfaces by covalently coupling 5 kDa PEG to single or multiple dihydroxyphenylalanine (DOPA) groups,[33] a catechol derivative that is present in interfacial MAPs in high concentrations (up to 27 mol %).[32] Assembled at cloud point conditions, high PEG surface densities could be achieved in combination with multiple DOPA anchors.[34,35] Various types of catechols have been studied in terms of their coordination to metals and metal oxides (Cu^{2+}, Fe^{3+} Ti^{3+}, Ti^{4+}, Mn^{2+}, Mn^{3+}, Zn^{2+}, Nb_2O_5, TiO_2)[35−40] and interaction with polymers (PTFE, PS, PDMS).[35] PEG linked to catechol derivatives such as DOPA, anacachelin chromophore, mimosine, and dopamine[41−43] have been compared with respect to their assembly properties and layer stability as well as resistance to oxidation in solution.

In the present work we hypothesized that a PEG-polyelectrolyte graft copolymer with part of the lysine side chains (amine groups) functionalized with catechol groups should combine the advantages of the electrostatically driven, spontaneous self-assembly and molecular organization of the polycationic PEG-copolymer on negatively charged surfaces with the high adhesion strength, kinetic inertness, and expected long-term stability of the multivalent catechol−surface anchorage concept. To this end, we prepared six PLL-*graft*-(DHPAA; PEG) copolymers with different fractions of 3,4-dihydroxyphenylacetic acid (DHPAA) grafted to the PLL backbone (Figure 1). In order to be able to efficiently test a matrix of adsorption and exposure parameters (polymer concentration, assembly temperature, ionic strength, and time), we used an array-based surface modification device ("SuMo device") recently developed in our group.[44] Titanium oxide-coated substrates were used in view of their application relevance in the field of titanium medical devices and high refractive index based optical (bio)sensors. Polymer adlayer formation was studied quantitatively using ellipsometry and in situ optical waveguide lightmode spectroscopy (OWLS). The degree of nonfouling character of the polymeric thin films was tested by incubation with (fluorescently labeled) fibrinogen (Fbg), a sticky plasma protein,[45] and in cultures of the cyanobacterium *Lyngbya sp.* for for up to 100 days.

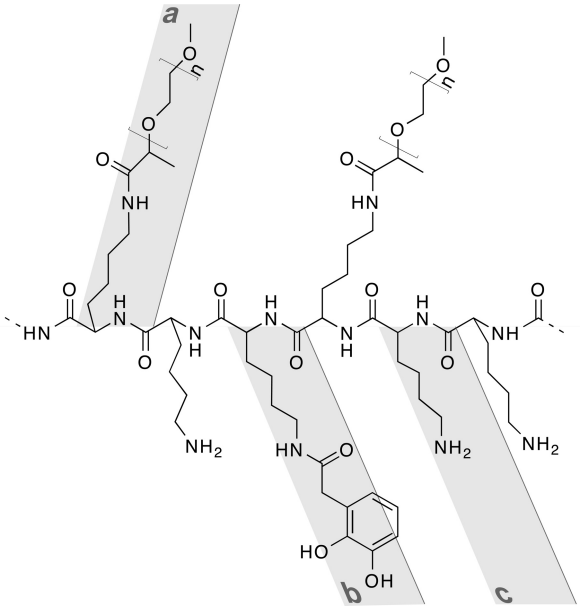

Figure 1. Chemical structure of the copolymer poly(L-lysine)-*graft*-(3,4-dihydroxyphenylacetic acid, poly(ethylene glycol) (PLL-*g*-(DHPAA; PEG) (20000:168:2000 M_r; 0−0.70:0.29 *d*). This abbreviation for the copolymers is defined in the Materials and Methods section. The three building blocks of the copolymer are PEG (a) and DHPAA (b), both conjugated to the amino group of the side chain of the lysine monomer (c) in the PLL backbone.

Materials and Methods

Substrates. Silicon wafer slides from POWATEC GmbH, Hünenberg, Switzerland, and microscopic glass slides from Menzel GmbH & Co. Braunschweig, Germany, were used as substrates, both types with dimensions of 76×26 mm^2. Optical waveguide chips with a $Si_{0.75}Ti_{0.25}O_2$ waveguiding layer were purchased from MicroVacuum Ltd., Budapest, Hungary.

All substrates were coated with a thin TiO_2 layer applied by reactive magnetron sputtering (PSI Villigen, Switzerland), with a coating thickness of 15−22 nm for the silicon wafer and glass slides and 6 nm for the waveguide chips.

Substrate Cleaning Procedure. The substrates were sonicated for 10 min each in toluene and twice in 2-propanol and dried under a stream of nitrogen. Subsequently, they were treated with oxygen RF plasma for 2 min (Plasma cleaner/sterilizer PDC-32G, Harrick Scientific Products Inc., Pleasantville, NY; pressure ≤0.025 mbar; power 100 W) and immediately assembled in the SuMo device.[44]

Standard Chemicals. Water of a Milli-Q system (Millipore, 18.2 Ω, TOC ≤ 5 ppb) was used for all experiments. Nitrogen of purity ≥99.999% was purchased from PanGas, Dagmarsellen, Switzerland; NaCl (99.5%) from J.T. Baker, Holland; 2-propanol, Lichrosolv, for gradient grade chromatography from Merck, Darmstadt, Germany; toluene, 99.8%, for HPLC from Acros Organics, VWR International Inc., West Chester, PA. Buffer: 4-(2-hydroxyethyl)piperazine-1-ethanesulfonic acid (HEPES, M_w: 238.30 g/mol) was purchased from Fluka Chemie AG, Switzerland.

Polymer Synthesis and Characterization. *a. PLL-g-PEG Starting Copolymer.* Poly(L-lysine)-*graft*-poly(ethylene glycol) (20000:2000 M_r; 0.29 *d*) abbreviated in the following as PLL-*g*-PEG, SuSoS AG, Dübendorf, Switzerland. The notation in the brackets ([*x*]: [a] M_r; [a] *d*) represents the molecular weight (M_r) in g/mol of PLL-HBr [x] and PEG [a], respectively, while [a] *d* represents the grafting density of PEG [a] (d_{PEG}) corresponding to the number of PEG side chains divided by the number of L-lysine monomers, which is equal to the inverted grafting ratio $1/g$.

b. PLL-g-(DHPAA; PEG). Six different graft copolymers poly(L-lysine)-*graft*-(3,4-dihydroxyphenylacetic acid; poly(ethylene

Table 1. Relationship between Equivalents of DHPAA Used in the Synthesis of the Seven Polymers and Observed Grafting Ratio[a]

polymer no.	1	2	3	4	5	6	7
targeted grafting density	0.00	0.05	0.1	0.2	0.3	0.5	0.7
DHPAA equivalents needed per PLL-*g*-PEG	0	4.8	9.6	19.2	28.8	48	67.2
DHPAA equivalents used per PLL-*g*-PEG in synthesis		23	46	91	182	361	729
excess factor		0.3	0.7	1.3	2.6	5.3	10.6
measured grafting density d_{DHPAA}(UV/vis)	0.00	0.08	0.09	0.16	0.26	0.46	0.70
DHPAA equivalents obtained per PLL-*g*-PEG	0	7.5	8.3	15.5	24.6	44.2	67.4
conversion efficiency [%]		33	18	17	14	12	9

[a] Assuming 96 free lysine units and 27 PEG chains per polymeric molecule ($d_{PEG} = 0.29$) corresponding to a total of maximum 69 free amino groups available for DHPAA grafting. The conversion efficiency is also tabulated.

glycol)) (20000:168:2000 M_r; [b]:0.29 *d*) in the following abbreviated as PLL-*g*-(DHPAA; PEG) ([b] d_{DHPAA}) were synthesized according to the protocol given below for one representative copolymer. The six polymers differed only in the DHPAA grafting density [b] d_{DHPAA}, which was varied between 0 and 0.7, whereas the grafting density of PEG [a] d_{PEG} remained constant at a value of 0.29. Polymers with the different grafting densities were achieved by varying the concentration ratio of DHPAA/PLL-*g*-PEG in the synthesis. The exact composition of the seven polymers is listed in Table 1.

Synthesis of PLL-*g*-(DHPAA; PEG) (20000:168:2000 M_r; 0.46:0.29 *d*). A solution of PLL-*g*-PEG (20000:2000 M_r; 0.29 *d*) (1.2 mL, 0.410 mM, 64.2 kDa) in HEPES 2 buffer (10 mM, pH = 7.4 and 150 mM NaCl) was prepared in a glass beaker and agitated with a magnetic stirrer. *N*-Ethyl-(3-diisoethylaminopropyl)carbodiimine (0.25 mL, 1 M, EDC, 155.24 g/mol, Fluka Chemie AG, Switzerland) and *N*-hydroxysuccinimide (0.25 mL of a 1 M, NHS, 115.09 g/mol, Fluka Chemie AG, Switzerland) separately dissolved in MQ water (0.25 mL each) were then mixed and immediately added to a solution of 3,4-dihydroxyphenylacetic acid (179.6 mM, DHPAA, 98%, M_w: 168.15 g/mol, ABCR GmbH & Co, Germany) in MQ water (1 mL). This mixture was then added dropwise to the well-stirred PLL-*g*-PEG solution and kept at room temperature for 18 h. The polymer was dialyzed (Spectra/Por dialysis membrane, MWCO: 12000−15000) against MQ water (4 L) that was exchanged three times. The final polymer solution was freeze-dried. Yield: 40.7 mg of a slightly yellowish fluffy powder. ^{1}H NMR (500 MHz, D_2O, ppm): 7.40 (s, 1H, DHPAA arom. on PLL N-terminus), 7.3 (q, 2H, DHPAA arom. on PLL N-terminus), 6.7 (q, 88H, arom), 6.6 (s, 44H, arom.), 4.2−3.8 (m, 96H, −HN−C*H*(CH−)−CO−), 3.7−3.4 (m, ≈4800H, −O−CH_2−CH_2−O−), 3.3 (s, 84H, −CH_2−CH_2−O−CH_3), 3.0 (m, 144H, −CH_2−CH_2−N−CO−), 2.7 (m, 48H, −CH_2−CH_2−NH_2), 2.3 (m, 27H, −CO−C*H*(CH_3)−O−and 88H, −C(arom.)−CH_2−CO−NH−), 1.7 (m, 144H, −O−NH−CH_2−CH_2−CH_2−), 1.6 (m, 48H, NH−CH_2−CH_2−CH_2), 1.35 (m, 192H, −NH−CH_2−CH_2−CH_2−CH_2−), 1.0 (d, 3H, −O−CH(CO−HN−)−CH_3).

Determination of the Grafting Density *d* of DHPAA. The grafting density of DHPAA (d_{DHPAA}) of the copolymer was determined with UV/vis spectroscopy by measuring the absorption of a 1.0 mg/mL PLL-*g*-(DHPAA; PEG) solution (in MQ water) at $\lambda_{max} = 280$ nm (Figure 2). The extinction coefficient ε was calculated by linear regression of a DHPAA absorption standard curve (0.001−1 mg/mL DHPAA in MQ water) to be 2.60 L/(mmol cm) at 280 nm. Because of the constant PEG grafting density (using the same batch of PLL-*g*-PEG as starting material), only the amount of DHPAA varied and thus enabled the calculation of the grafting density d_{DHPAA}. The PLL backbone of PLL-*g*-PEG (20000:2000 M_r; 0.29 *d*) consists of ∼96 L-lysine monomers, and a statistical amount of 27 L-lysine are linked to the PEG chains through the amino group in the side chains; therefore, 69 amino groups are still free. PLL-*g*-(DHPAA; PEG) (20000:168:2000 M_r; 0.30:0.29 *d*) contains 29 DHPAA molecules, 27 PEG chains, and 40 free NH_2. If d_{DHPAA} equals 0.71, there are 27 PEG chains, 69 DHPAA molecules, and 0 free NH_2.

Fibrinogen Labeling Procedure. Fibrinogen (40 mg, from human plasma, 35−65% protein (∼95% of protein is clottable), Sigma-Aldrich Co.) was diluted in sodium carbonate buffer (8 mL, 50 mM, pH = 9.0). Fluorescein isothiocyanate isomer **1** (0.25 mg, FITC, ≥90% HPLC, Fluka AG, Switzerland) dissolved in dimethyl sulfoxide (200 μL) was slowly added to the Fbg solution under continuous stirring and allowed to react for 1.5 h in the dark. The labeled protein was then dialyzed (Spectra/Por Dialysis membrane: MWCO: 3500, solvent: MQ water, 4× exchanged) for 18 h and subsequently freeze-dried (Alpha 1-2 LD plus, Martin Christ Gefriertrocknungsanlagen GmbH, Germany). Yield: 30 mg as fluffy yellow powder. UV/vis spectroscopy (Cary 1E instrument, Varian, Inc.): the absorbance of Fbg at 0.1 mg/cm^3 solution and at $\lambda_{max,Fbg} = 280$ nm was 0.2170, and the absorbance of FITC at $\lambda_{max,FITC} = 490$ nm was 0.2271 (extinction coefficient of 77000 M^{-1} cm^{-1}), corresponding to a statistical labeling rate of 11 FITC per Fbg.

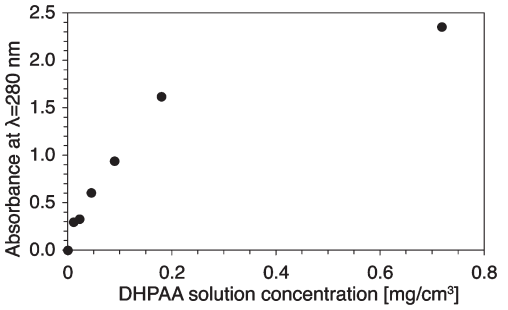

Figure 2. UV absorbance of the seven PLL-*g*-(DHPAA; PEG) polymers with increasing grafting density $d_{DHPAA} = 0-0.7$) as a function of the DHPAA solution concentration used for the reaction. All polymers were diluted in MQ water at a concentration of 1.0 mg/mL and measured at $\lambda_{max} = 280$ nm.

Polymer Adsorption Experiments in the SuMo Device. The SuMo device is a tool developed in our group[44] to perform 70 adsorption experiments in parallel on one substrate (26 × 76 mm^2). In brief, the 70-well plate was produced by clamping a punched silicone rubber sheet in contact with the substrate between two aluminum plates. Each well was filled with 20 μL of the polymer solution and incubated under the appropriate conditions. Adsorption experiments at higher temperatures were performed by placing the complete SuMo device in an oven (Bioblock Scientific, #45001). The wells were then rinsed with MQ water before disassembly, followed by a rinse in MQ water and blow-drying with nitrogen.

Fouling Test with FITC-Fbg. The complete slide was immersed in filtered (Minisart, cellulose, pore size: 0.2 μm, Sartorius Stedim Biotech, Aubagne Cedex, France) FITC-Fbg solution (15 mL, 0.1 mg/mL, in HEPES 2 (10 mM, pH = 7.4, 150 mM NaCl)). One of the wells was not exposed to the polymer solution and protected from FITC−Fbg adsorption by local application of Scotch tape; this well served later as a "zero" reference (black background) for the quantitative fluorescence measurements.

Evaluation of Inhibition of Aquatic Biofouling. Microscopic glass slides with the different polymer coatings were placed in plastic Petri dishes (10 mm × 900 mm), and sterile Zehnder medium for cyanobacteria[46] was added to fill two-thirds of the

Petri dish. The medium was then inoculated with a growing culture of the biofilm forming cyanobacterium *Lyngbya sp.* EAWAG 140. The cultures were incubated at room temperature under light from fluorescent tubes with light/dark cycle of 12:12 h for a period of 16, 28, and 100 days. For the 100 days experiment, sterile Zehnder medium was added after 70 days to compensate for evaporation. After the incubation period, the slides were first dipped in Zehnder medium to remove excess of biological material and then dried with a stream of N_2. Microscopic pictures were taken with an inverted microscope Leica DMI4000B equipped with a Leica DFC290 camera (Leica Microsystems GmbH, 35578 Wetzlar, Germany). Fluorescent pictures of the plate at 650 nm were obtained with a microarray scanner GenePix 4000B from Axon instruments/molecular devices/MDS Inc. (Sunnyvale, CA).

Ellipsometry. A spectroscopic microspot ellipsometer, SE850 (microspot focus ~200 μm spot size) from Sentech Instruments GmbH (Berlin, Germany) was used to measure the layer thickness of the adsorbed polymers and Fbg. Amplitude (Ψ) and phase (Δ) of the polarized light were measured at a single angle of 70° and in a spectral range of 350−900 nm. Each of the 70 wells was measured in the following sequence: bare TiO_2-coated silicon substrate, after polymer coating, and after Fbg incubation.

The Ψ and Δ curves were then fitted using the SpectraRay software (version #5728, Sentech Instruments GmbH), applying the following multilayer model: (a) 1 mm silicon (111, Jellison[47]); (b) 2.3 nm silicon oxide (Sellmeier layer, coefficients: $A_1 = 1.357230$, $A_2 = 0$, $A_3 = 1.3590120$, $B_1 = 0.0064010\ \mu m^2$, $B_2 = 0\ \mu m^2$, $B_3 = 93.2036440\ \mu m^2$); (c) titania (Tauc−Lorentz formulation for the dielectric constants (ε_1 and ε_2) with a band gap $E_g = 3.1915$ eV, peak transition energy $E_0 = 5.5994$ eV, broadening parameter $\Gamma = 8.3757$ eV, factor $A = -540.3$ eV); (d) polymer (Cauchy-layer, $n = 1.46$, $k = 0$ for $\lambda = 300-900$ nm); (e) fibrinogen (Cauchy layer, $n = 1.46$, $k = 0$ for $\lambda = 300-900$ nm); (f) air ($n = 1.000$). The optical parameters (n, k) of the titania layer were first fitted using the data of the bare TiO_2 and then kept constant during fitting of the polymer and protein layer thicknesses.

Fluorescence Readout. A fluorescence microarray scanner Tecan LS (Tecan AG, Switzerland) was used to measure the adsorbed FITC-Fbg (Cy3 filter, Ex543/Em575 nm, pixel resolution: 10 μm, two scans). The images were processed with IgorPro software (IgorPro, version 5.01 Carbon, WaveMetrics, Inc.); the 8-bit RGB TIFF file was imported and the gray value of the green channel (in case of FITC) displayed. The average gray value of each spot was then evaluated by a grid of circles (5 rows and 14 columns) that was fitted on the SuMo device spots (>2000 pixels per circle depending on the spot or the picture size). All gray values of the pixels located inside each circle were taken to determine the average gray value of the corresponding spot. The average gray values and standard deviations of each circle or spot were finally plotted in a table. Additionally, a threshold value was set in order to prevent high-intensity peak errors caused by agglomerates of Fbg or dust particles. It was fixed at 110% of the average gray value measured for the most intense spot on the slide (determined in a first evaluation without threshold set); for example, if 150 was the highest measured gray value, the threshold was set at 165.

Optical Waveguide Lightmode Spectroscopy (OWLS). Optical waveguide lightmode spectroscopy (OWLS, Micro Vacuum Ltd. Budapest, Hungary) is a label-free, grating coupler biosensor technique for the in situ investigation of molecular adsorption, by measuring the shift of the in-coupling angle, which is caused by changes of the refractive index at the sensor−solution interface. All adsorption experiments were performed at 25 °C on titanium oxide-coated (6 nm) optical waveguide sensors (Micro Vacuum Ltd., Budapest, Hungary).

Comparison of Results from OWLS and Ellipsometry Investigation. The dry thickness values measured by ellipsometry correlated reasonably well with the adsorbed mass per area measured in OWLS (Figure 3), confirming earlier findings published by Feuz et al.[48] The calibration curve allows us to transform the ellipsometric thickness values into adsorbed mass per unit area, assuming a homogeneous polymer film with a density corresponding to dry PEG (1.17 g/mL) neglecting the minor contribution of the PLL/DHPAA parts of the polymer.

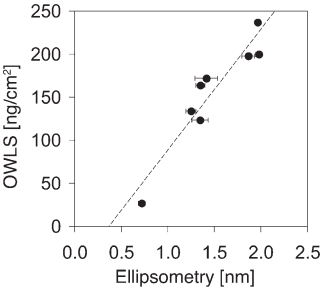

Figure 3. Correlation between the in situ adsorbed mass of the seven PLL-*g*-(DHPAA; PEG) copolymers, measured by OWLS (dry mass), with the thickness determined by ellipsometry in air. Polymer adsorption was performed at a concentration of 0.1 mg/mL in HEPES buffer with a concentration of 1, 10, or 100 mM and at room temperature (ellipsometry) or 25 °C (OWLS).

Results

Polymer Synthesis. The copolymers consist of poly(ethylene glycol) (PEG) and 3,4-dihydroxyphenylacetic acid (DHPAA) grafted to a poly(L-lysine) (PLL) backbone (Figure 1). Commercial available PLL-*g*-PEG was used as starting material for the synthesis of six additional copolymers with a varying DHPAA grafting density (d_{DHPAA} = number of DHPAA molecules/number of L-lysine monomers) from 0.08 up to 0.70. Because the same batch of PLL-*g*-PEG was used, the PEG grafting density remained constant ($d_{PEG} = 0.29$) for all copolymers. The grafting density of DHPAA (d_{DHPAA}) was varied and controlled by increasing the amount of DHPAA and corresponding activating agents in the synthesis protocol (Table 1). The relationship was not linear, though: the higher the targeted grafting density, the lower was the conversion efficiency of the reaction. To functionalize all free lysine groups, a 10-fold excess was needed. This was most probably due to increased steric hindrance and a competition between successful coupling and hydrolysis of the in situ generated active ester during the reaction. After completion of the reaction, excess reagents (DHPAA, NHS, EDC, and salts) were removed by dialysis and the products isolated by freeze-drying. The polymers were characterized by ^{1}H NMR and UV/vis spectroscopy. The absorbance of DHPAA at 280 nm allowed us to quantitatively determine the grafting density (d_{DHPAA}) of the polymers.

Polymer Adsorption. The influence of different assembly conditions on the adsorbed polymer mass and subsequent nonfouling properties (resistance to Fbg adsorption) of the polymer-coated samples was studied as a function of the DHPAA grafting density. Polymer adsorption was monitored by both ellipsometry (in air, dried films) and OWLS (in situ). TiO_2 as substrate and a polymer concentration of 0.1 mg/mL were used for all experiments, while adsorption time, ionic strength, and temperature were varied (Figure 4 and Figure S-1, Supporting Information). According to previously performed adsorption experiments with PLL-*g*-PEG on titanium oxide,[44] the following initial parameters were used: ionic strength of 10 mM HEPES, 1 h adsorption time, and room temperature.

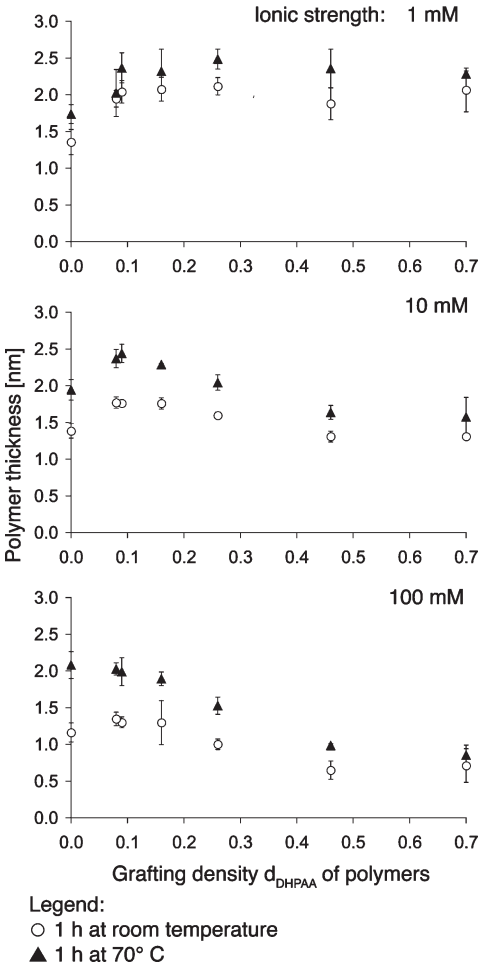

Figure 4. Polymer adlayer thickness of PLL-*g*-(DHPAA; PEG) copolymers with varying concentration of DHPAA grafted to the PLL backbone (*X*-axis). The polymers were adsorbed on TiO_2-coated silicon wafers as substrates from HEPES buffer (0.1 mg/mL) of increasing ionic strength (1, 10, and 100 mM top to bottom, pH = 7.4) at room temperature and 70 °C. Residual, unbound polymers were removed by a rinsing step and the adlayer then blow-dried. The thicknesses of the dried adlayer (*Y*-axis) were then measured with ellipsometry.

The variation of the incubation time from 1 to 17 h did not affect the adlayer thickness of any of the seven polymers. The adsorption of PLL-*g*-(PEG; DHPAA) copolymers with d_{DHPAA} = 0, 0.09, 0.46, and 0.7 was also measured in situ with OWLS. All curves showed saturation after 0.5 h of incubation but differed in their adsorption kinetics. The polymers with the higher grafting ratios adsorbed slower than pure PLL-*g*-PEG (Figure S-2, Supporting Information).

Figure 4 demonstrates that the ionic strength strongly influenced the polymer adsorption process. Polymers thickness was systematically lower if the assembly was carried out at higher ionic strength, particularly noticeable at higher d_{DHPAA} values; for the polymer with the highest DHPAA content (d_{DHPAA} = 0.7), the difference in polymer film thickness was 1.3 nm or almost a factor 2 when comparing the results for the 1 and 100 mM assembly conditions. The least affected was PLL-*g*-PEG (d_{DHPAA} = 0). In order to prove that this difference in adlayer thickness was caused by the ionic strength effect and not by the buffer system, the results for the different HEPES concentrations (1, 10, and 100 mM HEPES) were compared with those of a 1 mM HEPES buffer, to which sodium chloride was added at an overall ionic strength of 10 and 100 mM. No difference in adlayer thickness was observed, demonstrating that the effect was only caused by the ionic strength (Figure S-1, Supporting Information).

The second important parameter was found to be the adsorption temperature. Again, polymer thicknesses were systematically higher at the elevated assembly temperature of 70 °C compared to the RT results. In this case, the effect was more pronounced for polymers with low DHPAA content and more so at higher ionic strength. The most pronounced temperature effect was observed for PLL-*g*-PEG (d_{DHPAA} = 0) at 100 mM ionic strength. In general, the highest thickness values for the polymer adlayers were observed with DHPAA grafting densities in the range of 0.09−0.26 d_{DHPAA} (Figure 4).

Fouling Test with Fibrinogen. All polymer coatings were tested for their nonfouling properties with the sticky Fbg protein. It was chosen among three proteins (bovine serum albumine, fibronectin, and Fbg) because of the high layer thickness if adsorbed on titania (Figure S-3, Supporting Information). To this end, the substrate slide (76×26 cm^2), with which 70 different surface modification experiments were previously performed using the SuMo array device, was incubated in a 0.1 mg/mL FITC−Fbg solution. The level of adsorbed FITC−Fbg was determined with ellipsometry in terms of (additional) layer thickness and, in parallel, with a microarray scanner, for the adsorbed Fbg mass (after correction and calibration of the fluorescence intensities).

Figure 5 shows the normalized Fbg adlayer thicknesses adsorbed on the prior generated polymer adlayers, measured with ellipsometry. All thickness values were normalized against the average Fbg adlayer obtained on bare TiO_2 (set to 100%) and 0.0 nm as zero value (0%). The normalization allows a direct comparison of the experiments on different substrate slides and eliminates minor potential changes caused by slight variation of the protein solution (e.g., due to agglomerations, filtration, etc.). Figure 5 clearly demonstrates that the degree of Fbg adsorption on the polymer-coated surfaces depended on both the DHPAA concentration and the adsorption conditions (the latter presented in Figure 4). All PLL-*g*-(DHPAA; PEG) copolymer coatings successfully suppressed Fbg adsorption, if adsorbed at low ionic strength (1 mM). The Fbg adsorbed mass in these cases was below the detection limit of the ellipsometry assay.

Increased ionic strength (100 mM) during the polymer adsorption, however, resulted in enhanced Fbg adsorption for polymers with higher DHPAA grafting density (d_{DHPAA} > ca. 0.2). The amount of Fbg adsorption increased drastically with d_{DHPAA}. We also investigated whether increased incubation time in the polymer assembly step affected resistance to nonspecific Fbg adsorption. Rising adsorption time from the standard 1 to 17 h did not change the Fbg adsorption (Figure S-6, Supporting Information). Polymer adsorption temperature, on the other hand, significantly affected the level of Fbg adsorption to the polymer-modified surfaces. In comparison to the polymers assembled at room temperature, Fbg did not adsorb (below detection limit) to any of the PLL-*g*-(DHPAA; PEG) copolymer adlayers with a d_{DHPAA} up to 0.46, if adsorbed at 70 °C and from 1, 10, and 100 mM HEPES buffer. Only the polymer layer with d_{DHPAA} = 0.7 (adsorbed at 70 °C and from 10 or 100 mM HEPES) was not resistant to unspecific Fbg adsorption.

The adsorption of the PLL-*g*-(DHPAA; PEG) polymers with d_{DHPAA} of 0.09 and 0.46 and subsequent fibrinogen incubation were also investigated on TiO_2-coated waveguides using the in situ, real time OWLS technique at 25 °C (Figure S-7, Supporting Information). The data

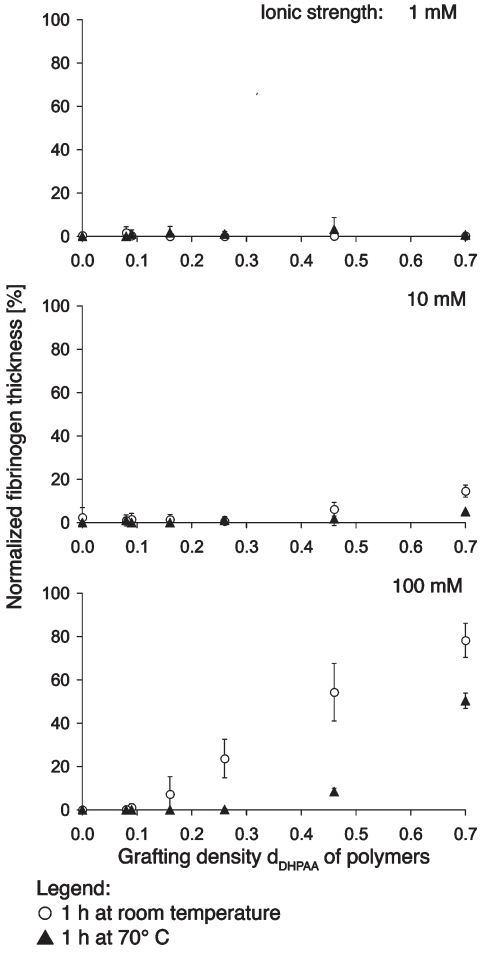

Figure 5. Normalized fibrinogen adlayer thickness (*Y*-axis) on TiO_2-coated silicon wafers, which were previously coated with PLL-*g*-(DHPAA; PEG) copolymer of varying DHPAA grafting density (*X*-axis, see Figure 3). The substrate was incubated in 0.1 mg/mL FITC−Fbg solution (HEPES 10 mM, pH = 7.4, 150 mM NaCl) for 1 h at room temperature. After rinsing and drying, the Fbg adlayer thickness was measured with ellipsometry and normalized with the Fbg adlayer thickness obtained on the bare TiO_2 control surface (= 100%) and 0.0 nm as "zero" reference (= 0%).

proved to be in good agreement with those of the ellipsometry measurements. The polymer with $d_{DHPAA} = 0.09$ systematically prevented the surface from adsorbing Fbg, independent of the ionic strength of the polymer adsorption solution (1−100 mM), in contrast to PLL-*g*-(DHPAA; PEG) with $d_{DHPAA} = 0.46$ for which the Fbg adsorbed mass increased with raising ionic strength.

An example of a fluorescence scanner image is displayed in Figure S-3 (Supporting Information); it shows the level of FITC-Fbg adsorption on all PLL-*g*-(DHPAA; PEG) copolymers ($d_{DHPAA} = 0-0.70$) adsorbed at 50 °C. Twenty-eight of the polymer adlayers were subsequently incubated in sodium chloride (5.3 M, overnight, at RT) in order to test the stability of the coating. The details of this assay are described in the section Polymer Adlayer Stability. The adsorption of FITC-Fbg was visible on the blanks but not on the copolymers, except on the salt-treated PLL-*g*-PEG coatings. Quantification was done by the determination of the average gray value on each spot and on the two reference spots, which were completely covered with Fbg and empty (bare TiO_2), respectively. The two references were used for the normalization of the FITC intensity and enabled the direct comparison of different experiments. The FITC

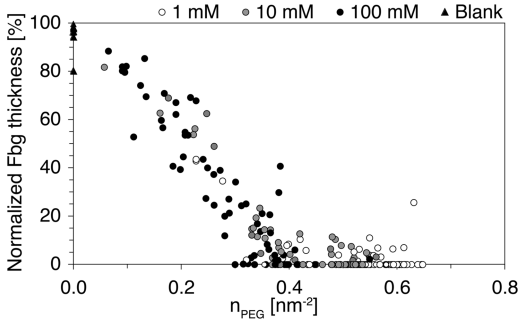

Figure 6. Normalized fibrinogen thickness (100% = value for bare substrate) plotted as a function of the number of surface-bound PEG chains per square nanometers. The values for the PEG chain surface density and Fbg-normalized thickness were calculated from the thickness of polymer and Fbg adlayer, respectively, both measured by ellipsometry. The seven PLL-*g*-(DHPAA; PEG) copolymers with a $d_{DHPAA} = 0-0.70$ were adsorbed at room temperature from HEPES buffer with an ionic strength of 1, 10, and 100 mM. To test the nonfouling properties of the polymer adlayers, SuMo arrays were incubated at room temperature in a solution of 0.1 mg/mL FITC-Fbg for 1 h.

intensity of the dry adlayer correlated with the FITC-Fbg layer thickness measured with ellipsometry (Figure S-5, Supporting Information), although slight differences can occur due to quenching effects.[44]

Correlation between Polymer and Fibrinogen Adsorption. PEG surface density (number of PEG chains per unit area) of the adsorbed polymer layers was plotted against the normalized FITC-Fbg thickness in Figure 6. The values refer to 1 h, room temperature adsorption and HEPES buffer with ionic strength values of 1, 10, and 100 mM. In order to compare the experiments performed on the three different substrates, and also to minimize effects caused by e.g. small variations of Fbg concentration, rinsing conditions, etc., the thickness values were normalized to the Fbg thickness obtained on the blank (not polymer-coated) reference spots of each slide (= 100% Fbg coverage), similarly as previously done with the FITC fluorescence intensity. The surface densities of PEG (2 kDa) chains were calculated from the (dry) polymer thickness values obtained by ellipsometry, a PEG density, $\rho_{dry\,PEG}$, of 1.17 g/mL, a grafting density, d_{PEG}, of 0.29 corresponding to 27 PEG chains per polymer molecule (N_{PEG}), and the molecular weight of the different polymers ($M_{r,polymer}$).

Adsorbed Fbg layer thickness was found to steadily decrease with increasing PEG surface density, reaching values that were generally below detection level for surface densities $n_{PEG} \geq 0.4$ PEG chains/nm^2. The latter value was similar to the minimally required n_{PEG} value of 0.44 PEG (2 kDa) chains/nm^2 obtained by Pasche et al.[28] for copolymers of the type PLL(20)-*g*-PEG(2) adsorbed on Nb_2O_5 (protein resistance tested against full serum).

$$n_{PEG} = \frac{A h_{ELM} \rho_{dry\,PEG} N_A N_{PEG}}{M_{r,polymer}}$$

where A = area, h_{ELM} = adlayer thickness ellipsometry, $\rho_{dry\,PEG}$ = density of dry PEG, N_A = Avogadro constant, N_{PEG} = number of PEG per molecule, and $M_{r,polymer}$ = molecular weight of the polymer.

Evaluation of the Inhibition of Aquatic Biofouling against *Lyngbya sp.* EAWAG 140. The long-term stability and antifouling properties of the polymers PLL-*g*-(DHPAA; PEG) (20000:168:2000 M_r; 0−0.70:0.29 *d*) were further tested with cultures of the biofilm-forming aquatic phototroph

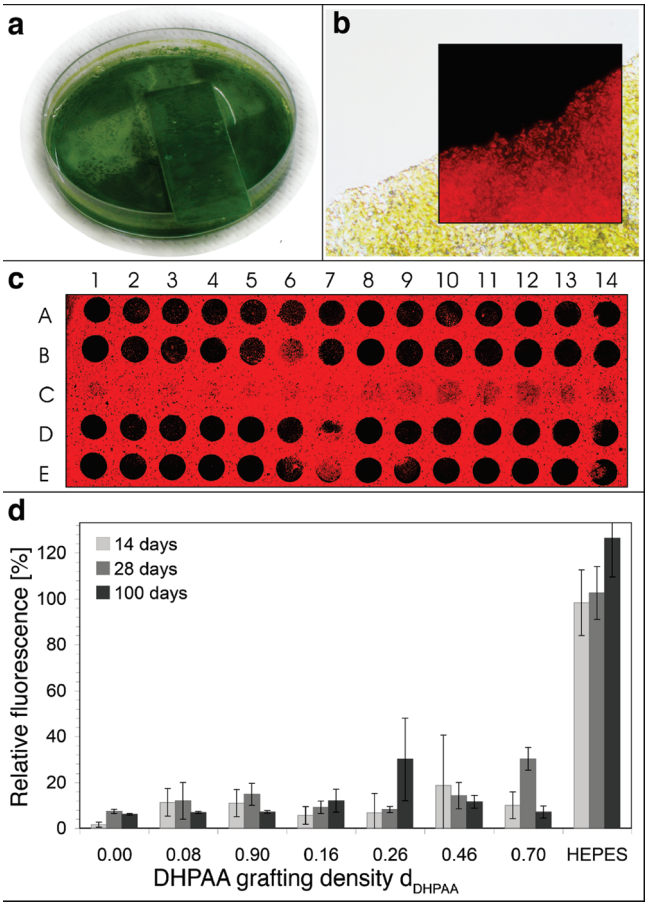

Figure 7. Fouling test with the cyanobacterium *Lyngbya sp.* EAWAG 140: Seven solutions of PLL-*g*-(DHPAA; PEG) copolymers with d_{DHPAA} = 0−0.70 (0.1 mg/mL in 10 mM HEPES, pH = 7.4) were adsorbed eight times at 70 °C on a titanium oxide-coated microscopy glass slide and then incubated in a Petri dish with cyanobacteria (a). The light microscopy image (b) displays the bacteria growth after 100 days on the bare TiO_2 (bottom right area) and the resistance on the polymer-coated spot (upper left area); the inset shows the red autofluorescence of the bacteria on the same spot. A complete fluorescence image of the slide incubated in cyanobacteria for 28 days was obtained with a microarray scanner (c). The polymers adsorbed on row A, B, D, and E had a grafting density d_{DHPAA} that decreased in columns 1−7 and 8−14 from 0.70 to 0.0. The spots of row C were left empty or filled with pure buffer and used as reference. Chart d displays the normalized fluorescence intensity measured on each spot/polymer for the different DHPAA grafting densities, plus the blank reference incubated only with HEPES buffer (right), and incubation times of 14, 28, and 100 days.

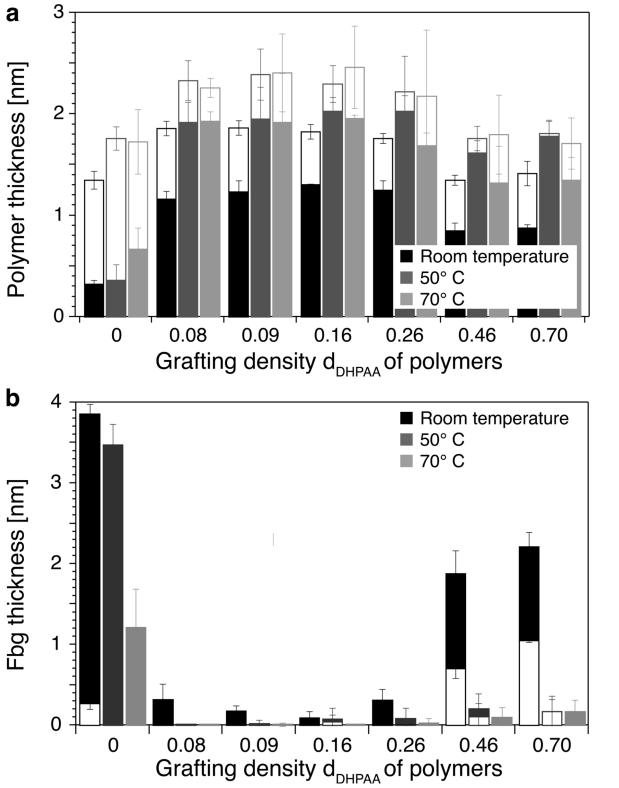

Figure 8. (a) Stability of the seven different PLL-*g*-(DHPAA; PEG) copolymers with increasing DHPAA grafting density d_{DHPAA} (*X*-axis). The polymers were adsorbed from 0.1 mg/mL solutions in HEPES buffer (10 mM, pH = 7.4) at room temperature (RT), 50 °C, and 70 °C on TiO_2-coated silicon wafer (framed bars). The solid bars display the polymer adlayer thickness (measured by ellipsometry) after the incubation in a 5.3 M sodium chloride solution for 17 h at RT. (b) Adsorbed Fbg ellipsometry thickness recorded on the polymer-coated surfaces with polymer thicknesses as displayed in (a). Substrate slides, each containing 70 polymer adlayers, were incubated in a 0.1 mg/mL Fbg solution for 1 h at room temperature. The framed bars show Fbg adsorption on the untreated and the solid bars Fbg adsorption on the salt-treated polymer coatings.

Lyngbya sp. EAWAG 140 (cyanobacteria, formerly called blue-green algae). Four titanium oxide-coated glass slides were assembled in the SuMo device and the 70 wells incubated with the different PLL-*g*-(DHPAA; PEG) polymers, dissolved in HEPES buffer (10 mM, pH = 7.4) at a concentration of 0.1 mg/mL and a temperature of 70 °C. *Lyngbya sp.* was then allowed to grow on the coated glass slide in a Petri dish for 16, 28, and 100 days (Figure 7a). Subsequently, the slides were dipped in Zehnder medium[46] to remove the excess of biological material and then dried with a stream of nitrogen. The autofluorescence of *Lyngbya sp.* allowed for selective evaluation of the presence or absence of biofilm formation with a microscope (Figure 7b) and a microarray scanner (Figure 7c) as well as to quantify relative coverage by the measurement of the average fluorescent intensity on the polymer-coated (and the bare control) spots (Figure 7d). Normalization of the determined absolute intensity values was required to compare the different surfaces; a similar procedure for the readout was applied as for the determination of the FITC-Fbg adsorption. The autofluorescence of the cyanobacterial film on blank, uncoated TiO_2-coated glass slides was taken as 100% relative intensity and zero absolute intensity as 0%. A dense, green cyanobacteria film was consistently formed across the whole glass slide, but simple dipping in culture medium released the bacteria film from the polymer-coated spots, but not from the bare (not polymer-coated) control spots. All seven copolymer coatings proved to resist cyanobacterial adsorption for a culture time of up to 100 days.

Polymer Adlayer Stability. The polymer adlayer stability test comprised the incubation of the coated substrates in saturated (5.3 M) sodium chloride (NaCl) solution for 17 h at room temperature. Polymer adlayer thickness and mass were measured before and after the salt treatment by ellipsometry (Figure 8) and OWLS (Figure S-7, Supporting Information), respectively.

Figure 8a displays the adlayer thickness of the polymer coatings measured with ellipsometry with different grafting ratio and adsorbed at room temperature, 50 °C, and 70 °C for 1 h in 10 mM HEPES buffer (pH = 7.4). The adsorption at higher temperatures resulted generally in increased layer thicknesses, but also in larger error bars, in comparison to the layers adsorbed at room temperature. However, a temperature of 50 °C was already sufficient to achieve a

significantly increased adlayer thickness. Adsorption at 70 °C led to no further increase of the adlayer thickness nor to further improved stability under high ionic strength conditions. The stability test with NaCl induced a strong reduction (from 1.73 to 0.67 nm at 70 °C) of the PLL-*g*-PEG adlayer adsorbed at either of the three temperatures. In contrast, for the polymers containing DHPAA, the reduction in adlayer thickness was less than 0.4 nm. This was already the case for the polymer with lowest DHPAA grafting density (d_{DHPAA} = 0.08 ≈ 7 DHPAA per polymer molecule).

Fbg was subsequently adsorbed on the polymer-coated substrates (0.1 mg/mL Fbg in HEPES 10 mM, pH = 7.4, 150 mM NaCl) for 1 h at room temperature (Figure 8b). Although the polymer films thickness of none of the PLL-*g*-(DHPAA; PEG) copolymers was tremendously reduced by the salt treatment, strong differences were observed in the subsequent Fbg adsorption. Especially the polymer coatings with a d_{DHPAA} higher than 0.26 provided no longer resistance to Fbg adsorption if assembled at room temperature ((1.9−2.2) ± 0.2 nm Fbg). If adsorbed at 50 or 70 °C, however, the adsorbed Fbg thickness was less than 0.2 nm, both without and with salt treatment of the polymer films.

The ellipsometry data were also compared with those of the OWLS investigation (Figure S-7, Supporting Information); PLL-*g*-(DHPAA; PEG) with values for d_{DHPAA} of 0.09, 0.46, and 0.79 and plain PLL-*g*-PEG were adsorbed for 0.5 h at 25 °C on TiO_2-coated waveguides by the injection of 0.1 mg/mL polymer solution in HEPES (10 mM), sufficient to reach saturation. A fraction of the polymer adlayers were subsequently treated with saturated NaCl solution due to instrumental limitation for only 0.5 h. This treatment was sufficient to strongly reduce the PLL-*g*-PEG layer thickness, albeit not as much as for the ellipsometry study where the exposure to high salt conditions was for 17 h (Figure S-8a). Finally, the nonfouling quality of the polymer adlayers was tested by the incubation of 0.1 mg/mL FITC-Fbg for 0.5 h. Low levels of Fbg adsorption (below 12 ng/cm^2) were recorded on all copolymer adlayers with d_{DHPAA} ranging from 0.09 to 0.26, while 306 ng/cm^2 of Fbg adsorbed to the salt-treated PLL-*g*-PEG adlayer (Figure S-8b).

Discussion

In the Introduction, we hypothesized that a (polyelectrolyte)-*graft*-poly(ethylene glycol) copolymer equipped with additional, covalently bound catechol groups could constitute a novel class of polymers that combines the advantages of polyelectrolytes,[28] i.e., spontaneous, electrostatically driven assembly and formation of dense, confluent layers at oppositely charged surfaces, with the strong and stable adhesion of biomimetic, catechol-based anchorage chemistry, derived from mussel adhesive proteins[33] or cyanobacterial siderophores.[22] We furthermore hypothesized that temperature and ionic strength of the assembly solution are likely to be important factors to consider, given the inverse temperature/solubility relationship of PEG and the dependence of polyelectrolyte solution conformation on ionic strength, respectively. The results achieved in this work and the following discussion provide evidence that this is the case.

a. Synthesis. A set of polymers with different grafting densities of DHPAA was successfully prepared using an easy, straightforward EDC/NHS-based conjugation protocol and commercially available starting materials, i.e., PLL-*g*-PEG with a Lys/PEG grafting ratio d_{PEG} = 0.29, optimal for achieving high PEG surface densities in the brush regime,[28,49] and 3,4-dihydroxyphenylacetic acid (DHPAA). The six different polymers were characterized with ^{1}H NMR, and the grafting density of the catechol function (d_{DHPAA}) was determined quantitatively by the absorbance at λ_{max}=280 nm using UV/vis spectroscopy. An important aspect for the following discussion is the relationship between the polycationic PLL backbone charge ($-NH_3^+$ groups) and the grafting density d_{DHPAA}. The higher the latter is, the lower the number of charges per molecule are, because the conjugation to DHPAA converts the free amine groups to an amide bond.

b. Polymer Adsorption Kinetics. The adsorption under standard conditions (0.1 mg/mL polymer in 10 mM HEPES buffer, 1 h, RT) of the PLL-*g*-PEG (20000:2000 M_r; 0.29 *d*) reference polymer, driven purely by electrostatic interaction, was fast as expected and reported in previous publications,[16,28] reaching saturation surface coverage within 15 min (Figure S-2, Supporting Information). 20 kDa PLL (as HBr salt) contains on average 96 free amines that are positively charged at pH 7, while for the standard PLL-*g*-PEG reference polymer 69 are free amines and 27 coupled to PEG via an (uncharged) amide bond.

For the PLL-*graft*-(DHPAA; PEG) copolymers with low DHPAA grafting density (d_{DHPAA} = 0.08−0.09, corresponding to an average of 8−9 DHPAA and 60−61 free amines per polymer molecule), the adsorption kinetics were similar to the reference PLL-*g*-PEG polymer (Figure 4 and Figure S-2, Supporting Information) but resulted in a slightly higher PEG chain density at saturation (0.38 vs 0.52 PEG chains/nm^2). The PLL backbone of these polymers obviously still contains a sufficient number of charges, resulting in fast, efficient adsorption and multiple charge interactions between the polycationic backbone and the negatively charged TiO_2 surface that can overcome the enthalpic and entropic penalty associated with the dense PEG chain arrangement in the surface-brush conformation.[49] The additional formation of concomitant strong DHPAA binding and associated gain in adsorption enthalpy is believed to be the reason for the observed higher PEG chain surface density achieved with this polymer in comparison to the control PLL-*g*-PEG.

A potential disadvantage of polymers with strong surface-anchorage groups could be the formation of irreversible binding and pinning of molecules as they arrive at the surface resulting in submonolayer formation (55% coverage at saturation in the random sequential adsorption model[50,51]). Judging from the excellent resistance to Fbg adsorption of TiO_2 surfaces coated with the low-DHPAA polymers (see below), this does not seem to happen, possibly related to the reversibility of the (strong) catechol−TiO_2 bond[52] and/or the easy conversion between the bidentate and the monodentate coordination site of catechols on surfaces as reported by Li et al.[53] This would be expected to allow for surface mobility of the adsorbed polymers, thus enabling the formation of a confluent, densely packed molecular layer.

The situation is entirely different for the polymer with very high DHPAA grafting density (d_{DHPAA} = 0.70), with only 2% of the PLL positive charge remaining (on average, this polymer has 67 DHPAA and 2 free (charged) amines per molecule). The adsorption kinetics was found to be much slower and the polymer coverage after 1 h of adsorption lower in comparison to the low DHPAA-*graft* polymer and PLL-*g*-PEG reference polymer (Figure S-2, Supporting Information). This observation is likely a consequence of the substantially reduced level of long-range attractive forces between the weakly charged polymer and the substrate surface. Adsorption for 17 h did not lead to a further increase in adsorbed mass or layer thickness (Figure S-1, Supporting Information), and the resulting surfaces were found, not surprisingly, to adsorb Fbg at levels well above the detection limit of the ellipsometry technique. Our interpretation of

these findings is related to results from self-consistent field calculations on PLL-*g*-PEG in solution approaching a negatively charged surface, experiencing an energy barrier that can only be overcome if "compensated" by a (long-range) attractive, electrostatic force.[49,54] The latter is no longer present in the polymer with $d_{DHPAA} = 0.70$, while the (necessarily short-range) coordination bond between the catechol groups (hidden by the PEG corona) and the titanium cations is expected to have a rather low probability of being formed under standard assembly conditions and realistic adsorption times.

c. Influence of Ionic Strength of the Assembly Solution. Variation of the ionic strength of the assembly solution turned out to have a major influence on the polymer film thickness and its degree of nonfouling character. Increasing ionic strength, from 1 to 100 mM, resulted in a general decrease of polymer layer thickness, and this effect was significantly more pronounced the higher the grafting density d_{DHPAA} was (Figure 4 and Figures S-1 and S-7 of Supporting Information). Correlated with this observation, the window of grafting densities d_{DHPAA} that resulted in low Fbg adsorption, varied drastically, from being very narrow (>0 to ≤ 0.1) to extending across the whole range of densities tested (0.1−0.7). The most obvious explanation relates to the screening of electrostatic interactions between the polycationic backbone and the negatively charged substrate surface with Debye lengths of approximately 10, 3, and 1 nm for ionic strength values of 1, 10, and 100 mM, respectively. Since 2 kDa PEG in water has a Flory radius $R_F \approx 2.9$ nm, the electrostatic field is expected to "shine out" of the PEG corona of a copolymer with bottle-brush conformation for ionic strength values <10 mM, thus resulting in important electrostatic, attractive interaction with the surfaces, which can overcome the steric PEG−PEG repulsion associated with the formation of a brush surface as discussed above.[49]

Another relevant factor could be related to the expected dependence of the copolymer conformation in solution depending on ionic strength. For the PLL-*g*-PEG system with higher PLL mol weight (300 kDa), it has been demonstrated that low ionic strength values of the assembly solution, favoring stretched out PLL conformation in solution, improves the favorable organization of the copolymers at the interface with the PLL backbone in close contact with the surface, while at higher ionic strength the formation of loops in the PLL backbone is likely to occur resulting in less well organized monolayers and reduced nonfouling properties.[54−56]

d. Effect of Assembly Solution Temperature. Increasing the adsorption temperature from RT to 70 °C resulted, for all grafting densities, in thicker polymer adlayers (Figures 4 and 8). The largest difference was observed for the polymers assembled from 100 mM HEPES buffer. The windows of grafting densities d_{DHPAA} for 50−70 °C polymer adsorption was correspondingly widened in comparison to RT assembly, most notably for adlayers assembled at 100 mM ionic strength (from $>0-\leq 0.1$ to $>0-0.3$).

There are two possible explanations to account for these findings, both of kinetic origin. First, the increased temperature is expected to increase the adsorption rate and stable organization of the copolymer at the interface, given the energy barrier of repulsive PEG interactions that has to be overcome during the assembly. Second, higher temperatures may be advantageous in terms of facilitating molecular reorganization of electrostatically preadsorbed polymers and formation of catechol−titanium coordination bonds.

e. Polymer Adlayer Stability. Exposure of the titania surfaces, coated with PLL-*g*-PEG and PLL-*graft*-(DHPAA; PEG) copolymers, to high salt (5.3 M NaCl) and subsequent Fbg solution was used in order to discriminate between electrostatic physisorption through the free lysine groups of the backbone and strong, coordinative binding of catechol group to titanium cations. This approach has been used before[31] in the context of probing adhesion strength of PLL-*g*-PEG with and without covalent attachment to aldehyde plasma polymerized layers.

PLL-*g*-PEG assembled polymers detached to a large extent during the high salt incubation step and showed subsequent Fbg adsorption levels comparable to the bare titania surfaces as expected. The stability performance of this copolymer was drastically altered by the presence of DHPAA ligands (Figure 8). Although there was some reduction in film thickness in the salt solution, possibly due to loss of some loosely bound polymers, most of the tested PLL-*graft*-(DHPAA; PEG) surfaces still preserved their nonfouling quality. Closely correlated with film thickness, the highest reduction of nonspecific fibrinogen adsorption was noticed for polymers with DHPAA grafting densities between approximately 0.1 and 0.3 and preferentially immobilized at the higher assembly solution temperatures, 50−70 °C.

Furthermore, the polymer layers successfully prevented attachment of the aquatic phototroph *Lyngbya sp*. in culture up to 100 days. Although cyanobacterial growth was observed on the complete surface, cyanobacteria did not adhere to the polymer-modified surfaces and were washed away upon dipping the substrate in medium. This was in stark contrast to the bare (non-modified titania surfaces), where cyanobacteria attached strongly. In view of the known formation of a bacterial biofilm,[57,58] including factors such as extra cellular matrix, polysaccharides, enzymes, etc., this excellent long-term stability was quite surprising. As after 100 d, there was still complete prevention of aquatic biofilm formation; experiments involving more strains, seawater, and a longer experimental time scale will certainly be of use in characterizing the scope of these polymers.

In summary, the class of PLL-*graft*-(DHPAA; PEG) copolymers was shown to be a useful addition to the toolbox of (bio-oriented) surface modification protocol in view of the simplicity of the application as a one-step, self-assembly process from aqueous solution, very low nonspecific adsorption when exposed to the (sticky) protein fibrinogen and long-term stability against attachment and colonization of cyanobacteria. Copolymer architectures optimized for achieving nonfouling properties and stability of surface-modified titania substrates are characterized by (a) a PLL/PEG (2 kDa) grafting ratio of ~3.5; (b) for assembly at room temperature, a DHPAA grafting density in the range of 0.1−0.2; and (c) for assembly at 50−70 °C, a DHPAA grafting density of 0−0.3 if assembled from 10 mM HEPES buffer.

Conclusion

The novel class of PLL-*graft*-(DHPAA; PEG) copolymers, presented in this work, was shown to be a valuable addition to the toolbox of surface functionalization protocols exploiting electrostatically driven self-assembly and concomitant strong, but reversible, adhesion based on biomimetic catechol−surface interaction. Design rules for this type of copolymer have been established covering both an optimum balance regarding the PEG/PLL grafting ratio, a sufficient number of (remaining) positive charge of the PLL backbone per molecule, and a minimum number of catechol binding moieties. Assembly conditions in terms of choice of assembly solution temperature and

ionic strength are crucial to achieve a well-controlled formation of a densely packed, nonfouling copolymer adlayer.

In view of the known ability of catechols to bind to a number of inorganic and a range of organic substrates, PLL-*graft*-(DHPAA; PEG) can be expected to be compatible with many different substrate compositions, notably metal oxides (e.g., transition metal oxides of zirconium, niobium, tantalum) as well as amine-presenting polymer films.[35] Furthermore, introduction of biofunctional ligands (biotin, peptides, carbohydrates, and others) at the termini of the PEG chains would be straightforward (possibly requiring modification of the DHPAA coupling scheme), opening up applications in fields such as bioaffinity sensors, cell culture substrates, and specific patterning of biomolecules, cells, or bacteria. Future potential research directions toward an even more universal binding approach may include expansion of the binding scheme to additional types of anchorage groups as well as applications to inorganic or amine-functionalized polymeric nano/microparticles for potential application in biomedical imaging and targeted drug delivery.

Acknowledgment. We thank the Swiss National Science Foundation for the support of this project (Grant 200021-112266). K.G. is a European Young Investigator (EURYI) and thanks the SNF for financial support (PE002-117136/1). Furthermore, we thank Dr. Silke Schön (FIRST, ETH Zurich, Switzerland) for access to the microspot ellipsometer, André P. Gerber (ETH Zurich Switzerland), Uwe Pieles, and Helmut Fally (FHNW Muttenz, Switzerland) for access to and technical support with the microarray scanner, Tobias Balmer (LSST, ETH Zurich, Switzerland) for help with the image evaluation program, and Professor Dr. Kai Johnsson (EPFL) for access to the microarray reader.

Supporting Information Available: Polymer adlayer thickness of PLL-g-(DHPAA; PEG) copolymers (Figure S-1); adsorption kinetics of the copolymers measured by OWLS (Figure S-2); layer thickness of three different proteins on TiO_2 as function of concentration (Figure S-3); fluorescence image of adsorbed FITC-Fbg (Figure S-4); adsorption of Fbg on the different copolymers (Figure S-5); fbg adlayer thickness as function of several adsorption conditions (Figure S-6); OWLS measurements of adsorption of PLL-g-(DHPAA, PEG) (Figure S-7); comparison of OWLS vs. ellipsometry data for the adsorbed polymer and fbg mass (Figure S-8). This material is available free of charge via the Internet at http://pubs.acs.org.

References and Notes

(1) Singh, R.; Dahotre, N. B. *J. Mater. Sci.: Mater. Med.* **2007**, *18*, 725–751.
(2) Bhushan, B.; Israelachvili, J. N.; Landman, U. *Nature* **1995**, *374*, 607–616.
(3) Castner, D. G.; Ratner, B. D. *Surf. Sci.* **2002**, *500*, 28–60.
(4) Ratner, B. D. *J. Biomed. Mater. Res.* **1993**, *27*, 837–850.
(5) Bhadra, D.; Bhadra, S.; Jain, S.; Jain, N. K. *Int. J. Pharm.* **2003**, *257*, 111–124.
(6) Currie, E. P. K.; Norde, W.; Stuart, M. A. C. *Adv. Colloid Interface Sci.* **2003**, *100*, 205–265.
(7) Swalen, J. D.; Allara, D. L.; Andrade, J. D.; Chandross, E. A.; Garoff, S.; Israelachvili, J.; Mccarthy, T. J.; Murray, R.; Pease, R. F.; Rabolt, J. F.; Wynne, K. J.; Yu, H. *Langmuir* **1987**, *3*, 932–950.
(8) Evans, S. D.; Ulman, A. *Chem. Phys. Lett.* **1990**, *170*, 462–466.
(9) Harder, P.; Grunze, M.; Dahint, R.; Whitesides, G. M.; Laibinis, P. E. *J. Phys. Chem. B* **1998**, *102*, 426–436.
(10) Ademovic, Z.; Klee, D.; Kingshott, P.; Kaufmann, R.; Höcker, H. *Biomol. Eng.* **2002**, *19*, 177–182.
(11) Brovelli, D.; Hahner, G.; Ruiz, L.; Hofer, R.; Kraus, G.; Waldner, A.; Schlosser, J.; Oroszlan, P.; Ehrat, M.; Spencer, N. D. *Langmuir* **1999**, *15*, 4324–4327.
(12) Gnauck, M.; Jaehne, E.; Blaettler, T.; Tosatti, S.; Textor, M.; Adler, H. J. P. *Langmuir* **2007**, *23*, 377–381.
(13) Tosatti, S.; Michel, R.; Textor, M.; Spencer, N. D. *Langmuir* **2002**, *18*, 3537–3548.
(14) Spori, D. M.; Venkataraman, N. V.; Tosatti, S. G. P.; Durmaz, F.; Spencer, N. D.; Zürcher, S. *Langmuir* **2007**, *23*, 8053–8060.
(15) Gao, W.; Dickinson, L.; Grozinger, C.; Morin, F. G.; Reven, L. *Langmuir* **1996**, *12*, 6429–6435.
(16) Kenausis, G. L.; Vörös, J.; Elbert, D. L.; Huang, N. P.; Hofer, R.; Ruiz-Taylor, L.; Textor, M.; Hubbell, J. A.; Spencer, N. D. *J. Phys. Chem. B* **2000**, *104*, 3298–3309.
(17) Bajpai, A. K. *Prog. Polym. Sci.* **1997**, *22*, 523–564.
(18) Blodgett, K. B. *J. Am. Chem. Soc.* **1935**, *57*, 1007–1022.
(19) Owen, M. J.; Williams, D. E. *J. Adhes. Sci. Technol.* **1991**, *5*, 307–320.
(20) Papra, A.; Gadegaard, N.; Larsen, N. B. *Langmuir* **2001**, *17*, 1457–1460.
(21) Fusetani, N. *Nat. Prod. Rep.* **2004**, *21*, 94–104.
(22) Gademann, K. *Chimia* **2007**, *61*, 373–377.
(23) Rovira-Bru, M.; Giralt, F.; Cohen, Y. *J. Colloid Interface Sci.* **2001**, *235*, 70–79.
(24) Konradi, R.; Pidhatika, B.; Mühlebach, A.; Textor, M. *Langmuir* **2008**, *24*, 613–616.
(25) Harris, J. M. *Poly(ethylene glycol) Chemistry Biotechnical and Biomedical Applications*; Plenum Press: New York, 1992.
(26) Harris, J. M. Poly(ethylene glycol) chemistry and biological applications developed from a symposium sponsored by the Division of Polymer Chemistry, Inc., at the 213th National Meeting of the American Chemical Society, San Francisco, CA, April 13−17, 1997.
(27) Kingshott, P.; Griesser, H. J. *Curr. Opin. Solid State Mater. Sci.* **1999**, *4*, 403–412.
(28) Pasche, S.; De Paul, S. M.; Vörös, J.; Spencer, N. D.; Textor, M. *Langmuir* **2003**, *19*, 9216–9225.
(29) Huang, N. P.; Michel, R.; Vörös, J.; Textor, M.; Hofer, R.; Rossi, A.; Elbert, D. L.; Hubbell, J. A.; Spencer, N. D. *Langmuir* **2001**, *17*, 489–498.
(30) Wattendorf, U. Towards receptor-specific targeting of antigen presenting cells with functionalized stealth microparticles. ETH Dissertation No. 17540; Federal Institute of Technology: Zurich, **2008** (doi: 10.3929/ethz-a-005582085).
(31) Blättler, T. M.; Pasche, S.; Textor, M.; Griesser, H. J. *Langmuir* **2006**, *22*, 5760–5769.
(32) Waite, J. H. *Integr. Comp. Biol.* **2002**, *42*, 1172–1180.
(33) Dalsin, J. L.; Messersmith, P. B. *Mater. Today* **2005**, 38–46.
(34) Dalsin, J. L.; Lin, L.; Tosatti, S.; Vörös, J.; Textor, M.; Messersmith, P. B. *Langmuir* **2005**, *21*, 640–646.
(35) Lee, H.; Dellatore, S. M.; Miller, W. M.; Messersmith, P. B. *Science* **2007**, *318*, 426–430.
(36) Rodriguez, R.; Blesa, M. A.; Regazzoni, A. E. *J. Colloid Interface Sci.* **1996**, *177*, 122–131.
(37) Araujo, P. Z.; Morando, P. J.; Blesa, M. A. *Langmuir* **2005**, *21*, 3470–3474.
(38) Martin, S. T.; Kesselman, J. M.; Park, D. S.; Lewis, N. S.; Hoffmann, M. R. *Environ. Sci. Technol.* **1996**, *30*, 2535–2542.
(39) Sever, M. J.; Wilker, J. J. *Dalton Trans.* **2004**, 1061–1072.
(40) Taylor, S. W.; Chase, D. B.; Emptage, M. H.; Nelson, M. J.; Waite, J. H. *Inorg. Chem.* **1996**, *35*, 7572–7577.
(41) Zürcher, S.; Wäckerlin, D.; Bethuel, Y.; Malisova, B.; Textor, M.; Tosatti, S.; Gademann, K. *J. Am. Chem. Soc.* **2006**, *128*, 1064–1065.
(42) Wach, J. Y.; Bonazzi, S.; Gademann, K. *Angew. Chem., Int. Ed.* **2008**, *47*, 7123–7126.
(43) Wach, J. Y.; Malisova, B.; Bonazzi, S.; Tosatti, S.; Textor, M.; Zürcher, S.; Gademann, K. *Chem.—Eur. J.* **2008**, *14*, 10579–10584.
(44) Saxer, S.; Pieles, U.; Elsener, M.; Horisberger, M.; Tosatti, S.; Textor, M.; Gademann, K.; Zürcher, S. *Prog. Org. Coat.* **2009**, DOI: 10.1016/j.porgcoat.2009.09.009.
(45) Fuss, C.; Palmaz, J. C.; Sprague, E. A. *J. Vasc. Interv. Radiol.* **2001**, *12*, 677–682.
(46) Staub, R. *Schweiz. Z. Hydrol.* **1961**, *23*, 82–98.
(47) Jellison, G. E. *Opt. Mater.* **1992**, *1*, 41–47.
(48) Feuz, L. On the Confirmation of Graft-Copolymers with Polyelectrolyte Backbone in Solution and Adsorbed on Surfaces. ETH Dissertation No. 16644, Federal Institute of Technology, Zurich, **2006** (doi: 10.3929/ethz-a-005210741).
(49) Feuz, L.; Leermakers, F. A.; Textor, M.; Borisov, O. *Langmuir* **2008**, *24*, 7232–44.

(50) Evans, J. W. *Rev. Mod. Phys.* **1993**, *65*, 1281–1329.
(51) Talbot, J.; Tarjus, G.; Van Tassel, P. R.; Viot, P. *Colloids Surf., A* **2000**, *165*, 287–324.
(52) Lee, H.; Scherer, N. F.; Messersmith, P. B. *Proc. Natl. Acad. Sci. U.S.A.* **2006**, *103*, 12999–13003.
(53) Li, S. C.; Wang, J. G.; Jacobson, P.; Gong, X. Q.; Selloni, A.; Diebold, U. *J. Am. Chem. Soc.* **2009**, *131*, 980–984.
(54) Feuz, L.; Leermakers, F. A. M.; Textor, M.; Borisov, O. *Macromolecules* **2005**, *38*, 8891–8901.
(55) Pasche, S. Mechanisms of Protein Resistance of Adsorbed PEG-Graft Copolymers. ETH Dissertation No. 15712, Federal Institute of Technology, Zurich, **2004** (doi: 10.3929/ethz-a-004843028).
(56) Feuz, L.; Strunz, P.; Geue, T.; Textor, M.; Borisov, O. *Eur. Phys. J. E* **2007**, *23*, 237–45.
(57) Blenkinsopp, S. A.; Costerton, J. W. *Trends Biotechnol.* **1991**, *9*, 138–143.
(58) An, Y. H.; Friedman, R. J. *J. Biomed. Mater. Res.* **1998**, *43*, 338–348.